APPLICATION OF POLYMER MATRIX COMPOSITE MATERIALS TO THE COMPONENTS OF MICRO-ELECTRO-MACHINE-SYSTEMS

Takayuki Kusaka*, Yasumitsu Iwase** and Masayuki Takagi**

** Department of Mechanical Engineering, Ritsumeikan University*
*** Graduate Student, Department of Mechanical Engineering, Ritsumeikan University*

SUMMARY: MEMS (Micro-Electro-Machine-System) has been expected as the fundamental technology of the next generation industries. The polymer materials are one of the most suitable materials for their good productivity and bio-compatibility in this field of engineering as well as silicone based materials. However, the polymer materials are rather disadvantageous in their mechanical properties such as elasticity, strength, fracture toughness, abrasion resistance, thermal expansion and dimensional stability. Hence, the carbon-fiber/polymer composite materials were applied to the components of MEMS to improve those mechanical properties. The experiments were mainly carried out using a composite system of CMF (Carbon Milled Fiber) and polyester resin. The experimental results demonstrated that the material system had excellent properties as structural material. Compounding the CMF of 130 μm into the polyester resin only by 10 %, Young's modulus was doubled, the fracture toughness increased by 80 % and the thermal expansion decreased by 50 %. However, the tensile strength decreased within the region of the volume content of carbon fibers up to 20 %. These trends were studied in detail on the basis of the rule of mixture and the numerical results of finite element analysis. The numerical results showed that the reduction of tensile strength was the consequence of the stress concentration at the end of the CMF. The size effect of the specimen was also investigated mainly on Young's modulus and tensile strength. However, it was not clear because the experimental error could not sufficiently negligible for the specimens of smaller size. A few parts of MEMS were fabricated by the photopolymerization process.

KEYWORDS: micro-scale structures, composite materials, short fibers, polymer matrix, mechanical properties, photopolymerization, MEMS

INTRODUCTION

Development of the micro- or nano-scale machines such as MEMS (Micro-Electro-Mechanical Systems), which is an interdisciplinary field involving mechanical, electrical, material and information engineering, is one of the most important tasks for the next generation [1,2]. Especially, the material science on micro-scale structures has been regarded as important since the latter half of the 1990s [3-5].

Various kinds of materials, such as metals, ceramics or polymers, are used in this field of engineering. Silicon-like materials have been used most frequently among them because of their workability via semiconductor processing technology. However, polymer materials have some advantages in cost, productivity and bio-compatibility to silicon-like materials despite their disadvantages in mechanical properties.

Reinforcement with high performance fibrous materials is an effective way to improve the mechanical properties of polymer materials. Especially, reinforcement with discontinuous fibers, which is suitable for mass and low-cost production, has been used in a lot of industrial applications. However, it is not easy to predict the efficiency of reinforcement with discontinuous fibers, because it can be affected by

some complex factors such as strength of interface or distribution of reinforcing fibers [6-9].

In the present work, feasibility on the application of discontinuous carbon fiber reinforced polymers to micro-scale structures was studied on the basis of classical theories and some experiments. In addition, fabrication of micro-parts with the discontinuous carbon fiber reinforced polymers was tried using the photopolymerization process [10,11].

MATERIALS

Materials

Table 1: Properties of materials.

Carbon milled fiber (MLD-300, Toray)				
Young's modulus	E_f	:	230	(GPa)
Tensile strength	S_f	:	3500	(MPa)
Diameter	$2R_f$	:	7	(μm)
Length	$2L_f$	:	130	(μm)

Polyester resin (27-751, Refine Tec)				
Young's modulus	E_m	:	2.1	(GPa)
Tensile strength	S_m	:	47	(MPa)
Poisson's ratio	ν_m	:	0.4	

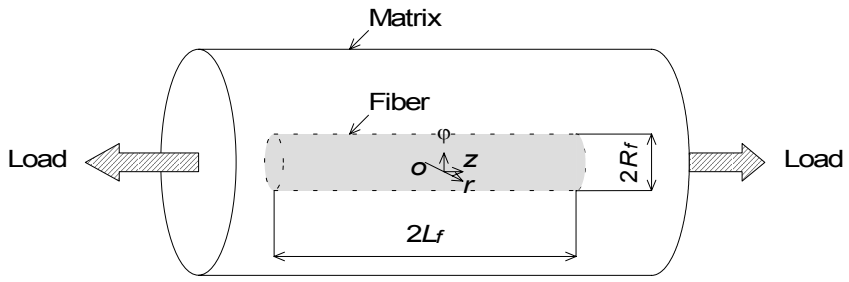

Fig. 1: Schematic drawing of the shear lag model subjected to an axial load.

A carbon-milled-fiber/polyester-resin composite material was used in the present work. The carbon milled fiber (MLD-300, Toray) is a PAN type discontinuous carbon fiber of 130 μm in average length, which is usually used for improving conductivity of rubber belts. The polyester resin (27-751, Refine Tec) is a two-component adhesive of room temperature setting type, which is usually used for making specimens for microscopic observation. The properties of materials are summarized in Table 1.

Specimens of fiber volume fraction, V_f = 0, 1, 2, 5, 10 and 20 %, were fabricated by the mold process using the carbon milled fibers and polyester resin with carefully defoaming at room temperature. The molding dies of stainless-steel for tensile specimens were fabricated with an electric discharge machine. Optical inspections were carried out to find out the existence of micro voids prior to the tensile tests.

Theoretical Prediction

The mechanical properties of short fiber composites can be predicted by the shear lag model [6-9]. In this model, a cylindrical shape of reinforcements is assumed as shown in Fig. 1, where R_f and L_f are

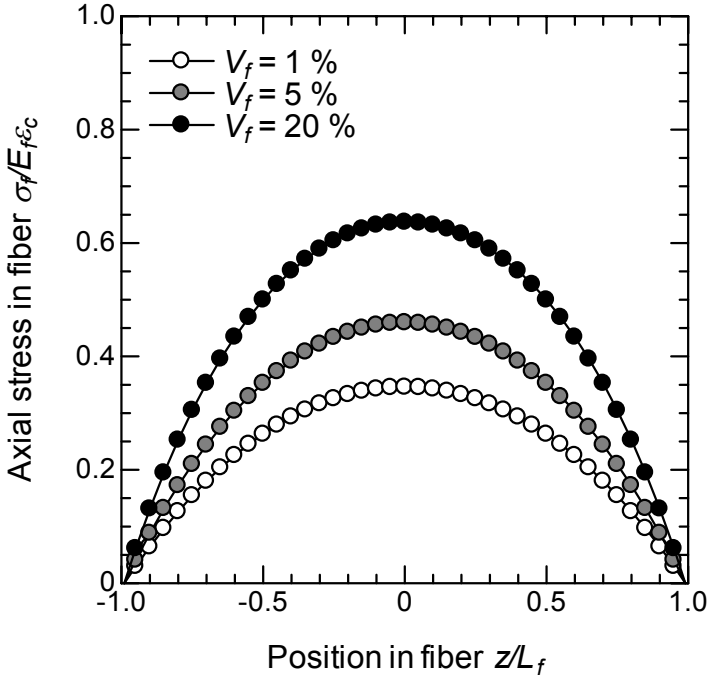

Fig. 2: Theoretical prediction of axial stress distribution in carbon milled fiber.

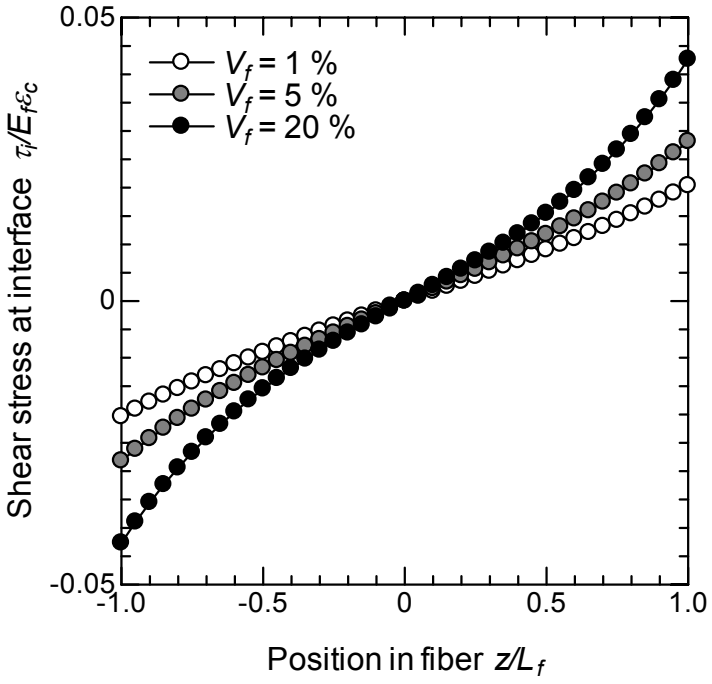

Fig. 3: Theoretical prediction of shear stress distribution at fiber/matrix interface.

the halves of diameter and length of the fiber.

On the basis of some considerations on equilibrium of forces acting on the fiber, the axial stress in the fiber, σ_f, and the shear stress at the interface, τ_i, can be written as a function of the position on fiber, z, [6];

$$\sigma_f = E_f \varepsilon_c \left(1 - \frac{\cosh(n z / R_f)}{\cosh(n s)}\right) \quad (1)$$

$$\tau_i = E_f \varepsilon_c \frac{n \sinh(n z / R_f)}{2 \cosh(n s)} \quad (2)$$

$$n = \sqrt{\frac{4 G_m}{E_f \ln(1/V_f)}} \quad ; \quad s = L_f / R_f \quad (3)$$

where E_f is Young's modulus of the fiber, G_m is the shear modulus of the matrix and V_f is the fiber volume fraction. ε_c is the overall strain of the composite in loading direction.

Figure 2 shows the distributions of the axial stress in the carbon milled fiber, σ_f, calculated by Eqn (1), parameterized with the fiber volume fraction, V_f. Figure 3 shows the distributions of the shear stress at the fiber/matrix interface, τ_i, calculated by Eqn (2), parameterized with the fiber volume fraction, V_f. The solid, shaded and open circles represent the predictions for the composites of 1, 5 and 20 % in fiber volume fraction, respectively. The material properties shown in Table 1 are used for the calculations.

The axial stress, σ_f, increases with increasing the fiber volume fraction, V_f, as shown in Fig. 2. However, the efficiency of reinforcement is about 24, 32 and 45 % of the continuous fiber composite on the average for the composites of V_f = 1, 5, 20 %, respectively. The shear stress, τ_i, also increases with increasing the fiber volume fraction, V_f, as shown in Fig. 3. However, the stress concentration at the end of fiber becomes higher for the composites of higher fiber content. This can lead to the reduction of overall tensile strength of the composite, which will be shown in the later section.

On the basis of the rule of averages, the apparent modulus of the composite, E_c, can be given by the following equation [6];

$$E_c = \eta E_f V_f \left(1 - \frac{\tanh(n s)}{n s}\right) + E_m (1 - V_f) \quad (4)$$

where η is the orientation efficiency factor [9]. It is estimated to be 1.00, 0.375 and 0.200 for the unidirectional (UD), two-dimensional random (2D) and three-dimensional random (3D) fiber distributions, respectively. The theoretical prediction by Eqn (4) will be compared with the experimental results in the latter section.

EXPERIMENTAL CHARACTERIZATION

Elastic Modulus

Static tensile tests were carried out to study the effects of fiber content and specimen size on elastic property of the material. Plate specimens of 0, 2, 5, 10 and 20 % in fiber volume fraction and 5.0 × 2.0, 2.0 × 0.5, and 0.5 × 0.2 mm^2 in sectional area were fabricated according to the JIS K7161. The strain rate was controlled at $d\varepsilon/dt = 10^{-2}$ 1/s.

Figure 4 shows the effect of the fiber volume fraction, V_f, on Young's modulus of the specimen, E_c, normalized by that of the matrix resin, E_m. The solid, shaded and open circles represent the results for the specimens of 5.0 × 2.0, 2.0 × 0.5 and 0.5 × 0.2 mm^2 in sectional area, respectively. The thin broken lines represents the theoretical prediction by Eqn (4) for unidirectional (UD), two-dimensional random

(2D) and three-dimensional random (3D) fiber distributions, respectively.

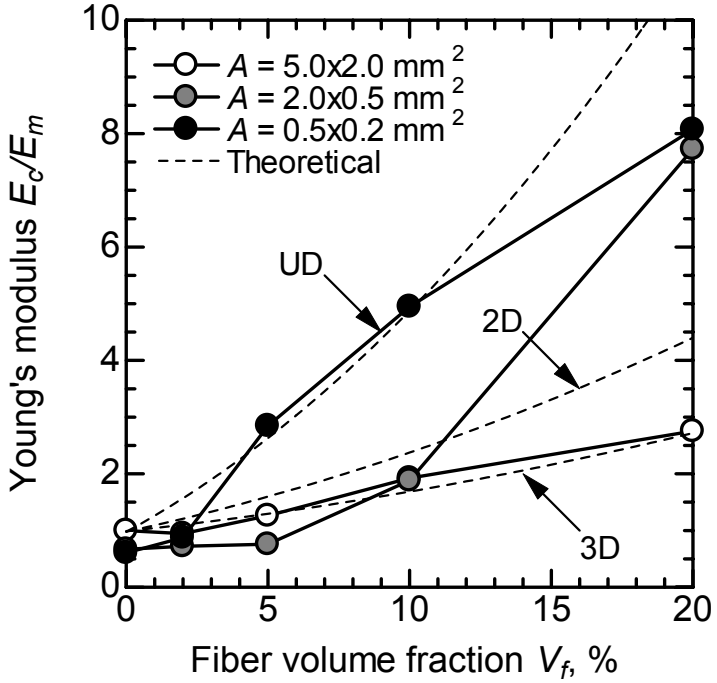

Fig. 4: Effect of fiber content on elastic property of the material.

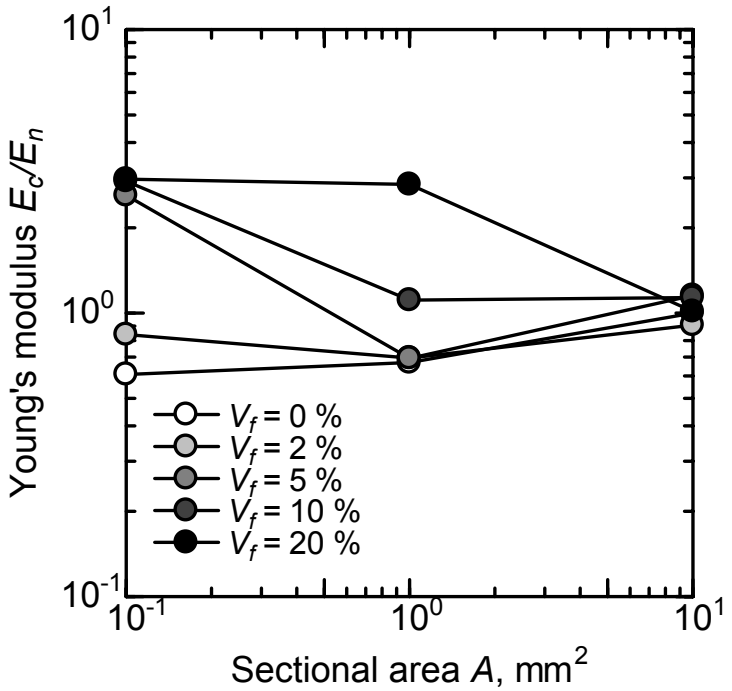

Fig. 5: Effect of specimen size on elastic property of the material.

As shown in the figure, Young's modulus of the specimen, E_c, increases with increasing the fiber volume fraction, V_f, regardless of the specimen size. For example, Young's modulus of the specimen, E_c, at V_f = 10 % is more than twice as large as that of the matrix resin, E_m. These results suggest that the reinforcement with carbon milled fibers is a very effective way to improve the stiffness of micro-

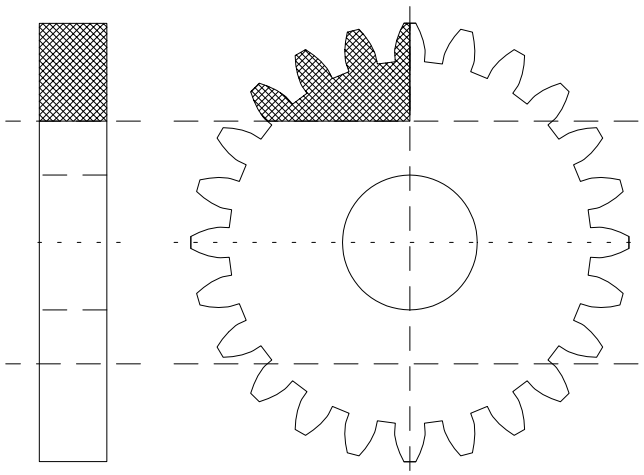

Particular sheet of micro-gear				
Module of gear	m_g	:	4	(μm)
Thickness of gear	t_g	:	100	(μm)
Diameter of pitch circle	d_g	:	960	(μm)
Number of teeth	Z_g	:	24	

Fig. 8: Schematic drawing of the micro-gear.

Table 2: Properties of photo-hardening polymer.

Urethane acrylate resin (DF-803N, Kayard)				
Young's modulus	E_p	:	2.6	(GPa)
Tensile strength	S_p	:	20	(MPa)
Mass density	ρ_p	:	1.1	(g/cm^3)
Surface tension	γ_p	:	0.023	(J/m^2)

parts made of polymer materials. However, the tendencies for the specimens of 2.0 × 0.5 and 0.5 × 0.2 mm^2 are quantitatively different each other. This may be the consequence of the difference of fiber orientation; smaller specimen size leads to a unidirectional fiber distribution, whereas larger specimen size leads to a random fiber distribution.

Figure 5 shows the effect of the sectional area, A, on Young's modulus of the specimen, E_c, normalized by that of the 5.0 × 2.0 mm^2 specimen, E_n. The solid, shaded and open circles represent the results for the specimens of 0, 2, 5, 10 and 20 % in fiber volume fraction, respectively.

As shown in the figure, Young's modulus of the specimen, E_c, largely increases with decreasing the sectional area, A, for the specimens of higher fiber content, whereas it approximately constant regardless of sectional area, A, for the specimens of lower fiber content. This may be also the consequence of the difference of fiber orientation; higher fiber content leads to a unidirectional fiber distribution, whereas lower fiber content leads to a random fiber distribution.

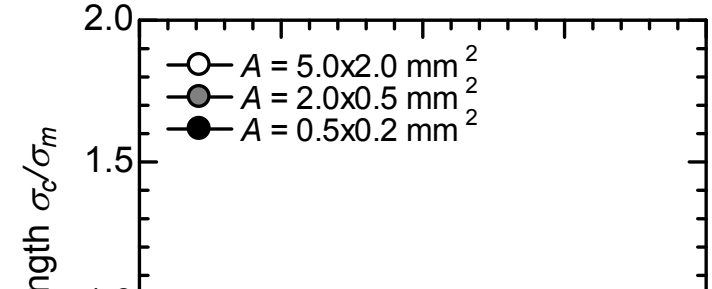

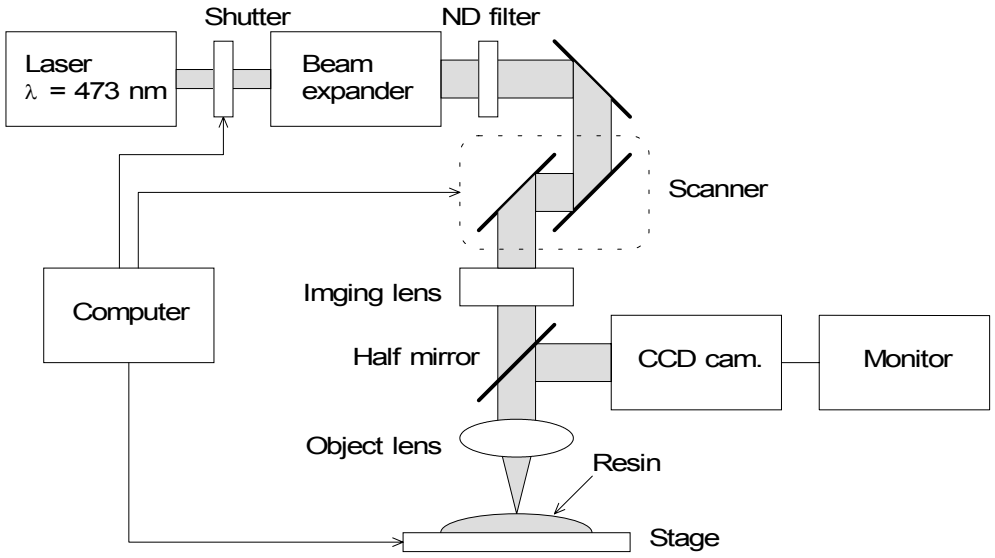

Fig. 9: Schematic drawing of the scanning beam photopolymerization apparatus.

Tensile Strength

Figure 6 shows the effect of the fiber volume fraction, V_f, on the tensile strength of the specimen, σ_c, normalized by that of the matrix resin, σ_m. The solid, shaded and open circles represent the results for the specimens of 5.0 × 2.0, 2.0 × 0.5 and 0.5 × 0.2 mm^2 in sectional area, respectively.

As shown in the figure, the tensile strength of the specimen, σ_c, does not significantly depend on the fiber volume fraction, V_f, regardless of the specimen size. However, the disturbance of the experimental results increased with decreasing the specimen size.

Figure 7 shows the effect of the sectional area, A, on the tensile strength of the specimen, σ_c, normalized by that of the 5.0 × 2.0 mm^2 specimen, σ_n. The solid, shaded and open circles represent the results for the specimens of 0, 2, 5, 10 and 20 % in fiber volume fraction, respectively.

As shown in the figure, the tensile strength of the specimen, σ_c, slightly decreases with decreasing the sectional area, A, regardless of the fiber content. The cause of this tendency has not been clear yet, though the plastic behavior of the matrix resin may depend on the specimen size.

FABRICATION OF MICRO-PARTS

Experimental Procedures

Figure 10 shows the drawing and particular sheet of the micro-gear, which is basically a standard involute gear, fabricated by way of trial. The number of teeth and diameter of pitch circle are 24 and 960 μm, respectively. The module and thickness of the gear are 4 and 100 μm, respectively.

The scanning beam photopolymerization process [11], which is suitable for test fabrication of micro-parts, was employed to fabricate the micro-gear, though the molding process with a die fabricated by the LIGA process was primarily planned to be employed. Hence, a carbon-milled-fiber/photo-hardening-polymer composite was temporarily used instead of the carbon-milled-fiber/polyester-resin composite. The photo-hardening polymer (DF-803N, Kayard), which has a larger reactivity than the

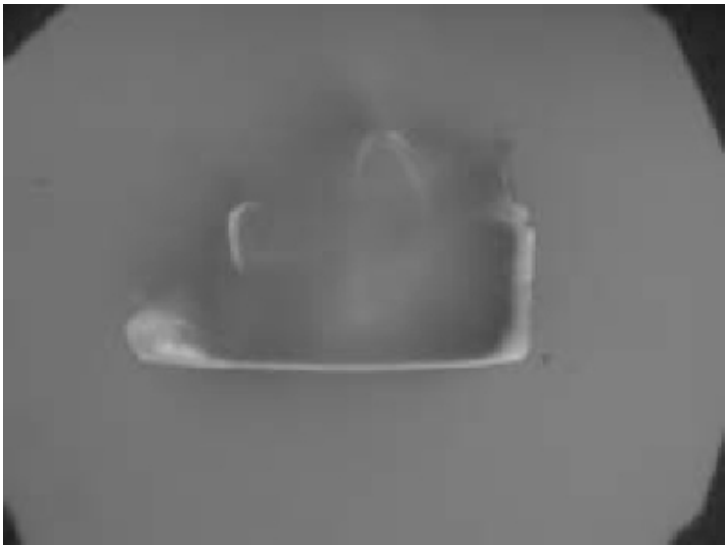

Fig. 10: Element of micro-gear fabricated by the photopolymerization process.

epoxy type resin, is a urethane acrylate type resin polymerized via a radical reaction by ultraviolet rays. The properties of photo-hardening polymer are summarized in Table 2.

The experimental apparatus used in the present work has a laser source of 473 nm in wave length and 14 mW in rated output, a beam scanner of 1.0 μm in scanning resolution and 25 μm in scanning speed, and a control unit, as shown in Fig. 11. However, the micro-gear had to be fabricated with dividing into eight elements owing to the limitation of scanning area, $500 \times 200\ \mu m^2$, of the current system, as shown in Fig. 10.

Experimental Results

Figure 12 shows the element of micro-gear, which corresponds to the hatched region in Fig. 10, fabricated by the scanning beam photopolymerization process. However, the carbon milled fibers are not involved in the element.

As shown in the figure, almost the complete shape of the element could be fabricated by the scanning beam photopolymerization process in case where the carbon milled fibers were not involved. However, the complete shape of the element could not be obtained owing to the disturbance of rays in case where the carbon milled fibers were involved. Also, the dimensions of carbon milled fibers were too large for the fabrication of divided elements. Hence, some other trials are now carried out using a carbon whisker of similar aspect ratio.

CONCLUSIONS

In the present work, feasibility on the application of discontinuous carbon fiber reinforced polymers to micro-scale structures was studied on the basis of classical theories and some experiments. In addition, fabrication of micro-parts with the discontinuous carbon fiber reinforced polymers was tried using the photopolymerization process. The results are summarized as follows;

(1) The theoretical prediction suggested the feasibility on the application of discontinuous carbon fiber reinforced polymers to micro-scale structures.

(2) The experimental results showed that the elastic modulus could be largely improved by the reinforcement with discontinuous carbon fibers.

(3) However, the experimental results showed that the tensile strength could not be improved in case of the material system used in the present work.

(4) The fabrication of a micro-gear of a discontinuous carbon fiber reinforced polymer did not succeed completely owing to the limitation of the current system.

This work was partly supported by a Grant-in-Aid for Scientific Research of the Ministry of Education, Culture, Sports, Science and Technology, Japan (Incentive Research (A), No.12750084). The fabrication of micro-parts was carried out under many helps of Prof. Ukita and members of his laboratory. Our special thanks are due to the related persons and organizations for their assistants.

REFERENCES

[1] M. Gad-El-Hak, *The MEMS Handbook*, CRC Press, Boca Raton (2001).
[2] T.R. Hsu, *MEMS and Microsystems; Design and Manufacture*, McGraw-Hill Science, New York (2001).
[3] K. Komai, "Current Needs and Future Trends of Micromaterials", *Journal of the Society of Materials Science, Japan*, 46-12 (1997), pp.1442-1447, (in Japanese).
[4] S. Kamiya, M. Saka and H. Abe, "Simulations for the Properties and Fracture Behavior of Micromaterials", *Journal of the Society of Materials Science, Japan*, 47-1 (1998), pp.100-105, (in Japanese).
[5] K. Komai, K. Minoshima and S. Inoue, "Fracture and Fatigue Behavior of Single Crystal Silicon Microelements and Nanoscopic AFM Damage Evaluation", *Microsystem Technologies*, 5 (1998), pp.30-37.
[6] D. Hull and T.W. Clyne, *An Introduction to Composite Materials, 2nd Ed.*, Cambridge University Press, Cambridge (1996), Chap.6.
[7] H.L. Cox, "The Elasticity and Strength of Paper and Other Fibrous Materials", *British Journal of Applied Physics*, 3 (1952), pp.72-79.
[8] H. Fukuda and T.W. Chou, "An Advanced Shear Lag Model Applicable to Discontinuous Fiber Composites", *Journal of Composite Materials*, 15 (1981), pp.79-91.
[9] H. Krenchel, *Fibre Reinforcement*, Akademisk Forlag, Copenhagen (1964), Chap.10.
[10] H. Kodama, "Automatic Method for Fabricating a Three-Dimensional Plastic Model with Photo-Hardening Polymer", *Review of Scientific Instruments*, 52 (1981), pp.1770-1773.
[11] H. Ukita, "Micromechanical Photonics", *Optical Review*, 4-6 (1997), pp.623-633.